

# Optical, structural and optoelectronic properties of pulsed laser deposition PbS thin film

D.M.M. Atwa · I.M. Azzouz · Y. Badr

Received: 19 May 2010 / Revised version: 8 September 2010 / Published online: 24 November 2010  
© Springer-Verlag 2010

**Abstract** Lead sulfide (PbS) nano-structured film has been grown on quartz substrates by the PLD technique. The deposited films were characterized by X-ray diffraction (XRD), selected area electron diffraction (SAED), transmission electron microscopy (TEM) and scanning electron microscopy (SEM). Formation of cubic phase of PbS nanocrystals is proven. The absorption and emission spectra were measured for different thicknesses of the films.  $I-V$  characteristics and photoconductivity of the deposited film were also measured. The results indicate an efficient performance of the deposited films as an optical detector.

## 1 Introduction

In recent years there has been increasing interest in the nano-structured and especially nano-structured semiconductors thin films. They are in an outstanding situation in the basic research and solid-state technology due to their future applications in quantum and photonic devices. PbS is an important intrinsic semiconductor material because of its various technological applications such as IR detectors [1, 2], photography [3], photo-thermal conversion and solar absorber [4, 5], optical amplification [6], sensors [7], luminescent display devices [8], and optical switches [9, 10]. PbS exhibits a narrow bulk direct band gap of 0.41 eV, which can be manipulated by miniaturizing the material dimensions. Due to the importance of PbS, the deposition of thin films on different substrates has been reported via several techniques, such as e-beam evaporation [11], molecular beam

epitaxy (MBE) [12, 13], successive ionic layer adsorption and reaction (SILAR) [14–16], electrodeposition [17, 18], hydro-chemical deposition [19], spray pyrolysis [20], chemical bath deposition (CBD) [21, 22] and pulsed laser deposition (PLD) [23–27]. The latter technique has the advantage of controlling the film's thickness with the maintaining of the target stoichiometry in the deposited layer. In 1997, PbS films were grown on glass substrates by laser ablation of Pb target in  $H_2S$  ambient gas [23]. Vaitkus et al. [24] have successfully grown PbS thin films on misoriented Si and NaCl substrates by laser ablation of PbS crystal. Additional structures of Pb core levels were observed. PbS thin-film sensors on the basis of different glass materials (PbS–AgI–AsS, CdS–AgI–AsS, Tl–Ag–As–I–S) have been prepared by means of an off-axis PLD [25]. It was shown that the complex stoichiometry of the chalcogenide target materials was maintained in the chalcogenide films. Recently, Dhlamini et al. [26] have successfully grown nanoparticles PbS films embedded in an amorphous silica host on Si substrates by PLD. The SEM data proved the agglomeration of spherical nanoparticles. The size of the nanoparticles was found to increase with the deposition temperature. Kumar and Chandra [27] has reported the PLD of PbS films on corning glass substrates. The surface morphology showed some spherical agglomeration. Increasing the laser flux density resulted in too coarsening and non-uniformity of particle size which increased the surface roughness of the film.

In the present work, we report the deposition of magic-square-shape nanocrystal PbS thin films by PLD technique. The morphology and crystal structure of the films was obtained by transmission and scanning electron microscope, selected area electron diffraction (SAED) and X-ray diffraction. The photo-conductive properties of the PLD thin films, in addition to the effect of the nano thickness on the absorption and emission properties of the films are reported.

D.M.M. Atwa · I.M. Azzouz (✉) · Y. Badr  
National Institute of Laser Enhanced Sciences, Cairo University,  
Giza 12613, Egypt  
e-mail: iftazzouz@niles.edu.eg

**Fig. 1** XRD of PbS film grown on quartz substrate at  $T = 350^{\circ}\text{C}$

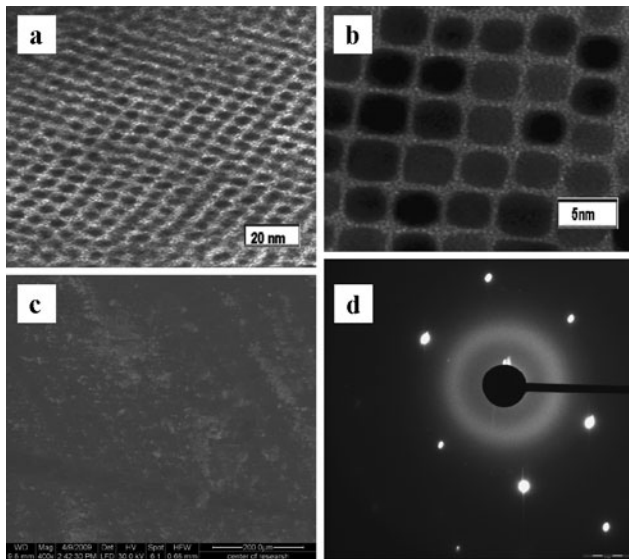
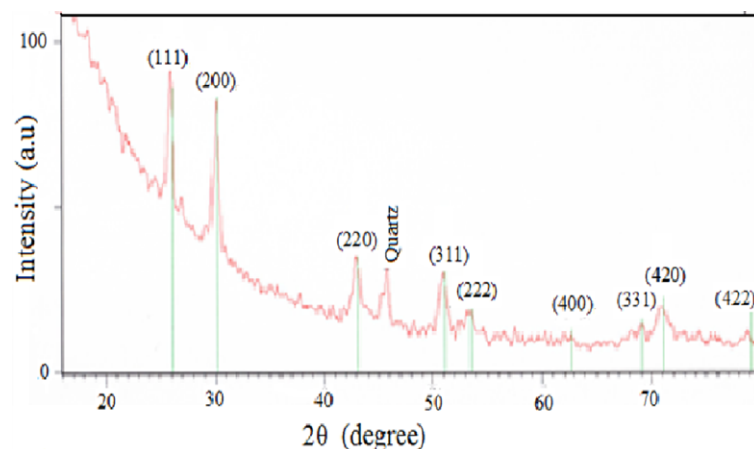


**Fig. 2** (a) TEM image (scale bar 20 nm), (b) localized TEM image (scale bar 5 nm), (c) SEM image and (d) SAED pattern of PbS nanostructure deposited on quartz substrate

Although the thin films obtained may have several applications, the main goal of this study was of a basic nature to produce efficient PbS thin film.

## 2 Experimental

The UV-PLD was performed with a XeCl excimer laser operating at 308 nm. PbS films were deposited on quartz substrates by ablating the pure PbS galena target (the common PbS mineral of cubic crystal structure). The target-to-substrate distance was 5 cm. The substrate temperature and ambient pressure were kept at  $350^{\circ}\text{C}$  and  $5 \times 10^{-5}$  torr, respectively. The samples were deposited using a laser energy density of  $2.5 \text{ J/cm}^2$  at a repetition rate of 100 Hz and ablation durations of 2.5 and 4 min. The film's thickness was measured by an optical interferometer. No post-deposition

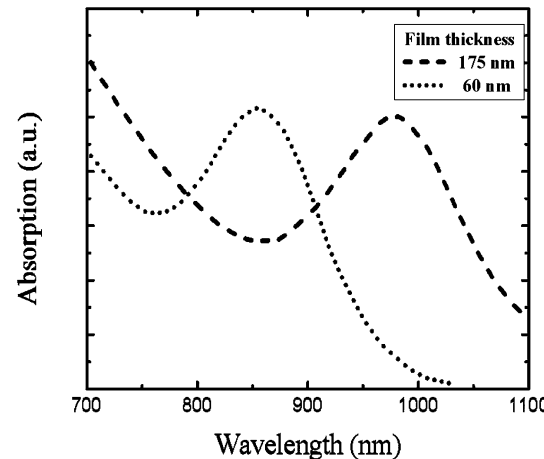


**Fig. 3** Absorption spectra of the deposited PbS films of thicknesses 60 nm and 175 nm

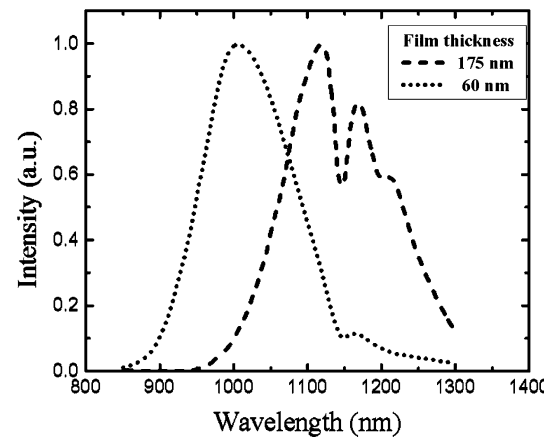
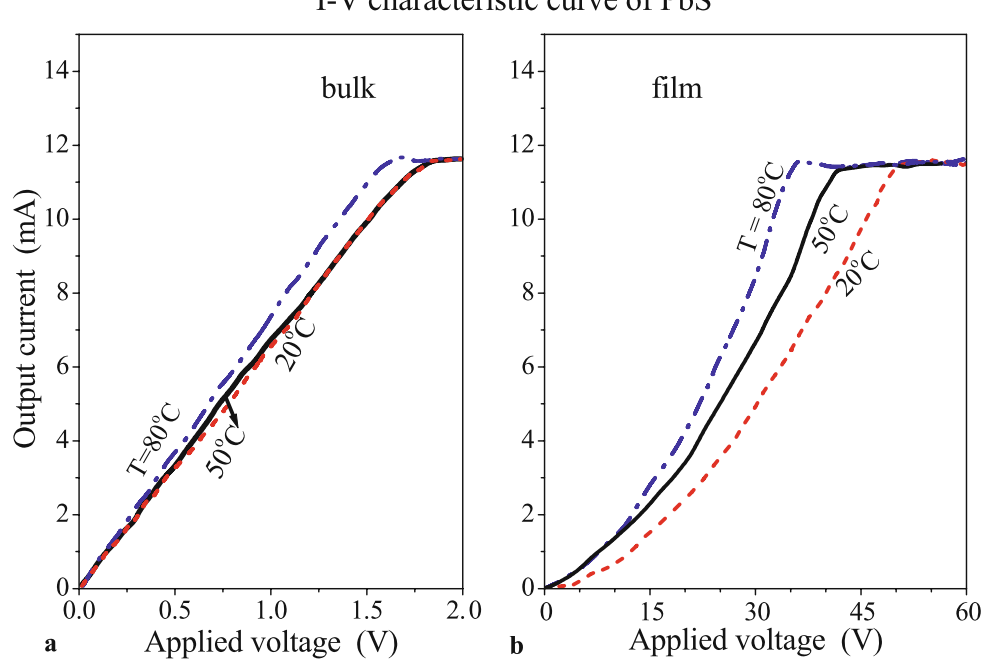


**Fig. 4** Photoluminous spectra of the deposited PbS films of thicknesses 60 nm and 175 nm

annealing was performed. The crystal structure of the deposited films was characterized by X-ray diffraction (XRD) using PRO pw 3040/60 (PANalytical) advanced X-ray diffractometer with  $\text{CuK}\alpha$  ( $\lambda = 1.54 \text{ \AA}$ ) radiation. The particle

**Fig. 5**  $I-V$  characteristic curves of PbS samples, in case of (a) bulk target and (b) deposited films, at temperatures values of  $20^{\circ}\text{C}$ ,  $50^{\circ}\text{C}$  and  $80^{\circ}\text{C}$



size and surface morphology was studied using transmission electron microscope (LIBRA 200 FE Zeiss) and scanning electron microscopy (FEI Quanta 3D 200i). The optical properties of the nanoparticles were measured using Perkin Elmer UV–Visible spectrophotometer. Also, the  $I-V$  characteristic curve of the deposited film was measured at different values of temperatures and compared to that of the bulk target. The result of applying the prepared film as a sensor for the NIR radiations is also presented.

### 3 Results and discussion

Figure 1 shows the XRD pattern of the deposited PbS film on the quartz substrate. The diffraction peaks can be indexed to the planes (111), (200), (220), (311), (222), (400), (331), (420) and (422) of the cubic crystal phase of PbS with the calculated lattice constant  $a = 5.936 \text{ \AA}$ . The plane spacing “ $d$ -values” are calculated from Bragg’s relation:  $2d_{hkl} \sin\theta = n\lambda$  (for  $n = 1$  and  $\lambda = 1.54 \text{ \AA}$  the wavelength of X-ray).  $\theta$  is the diffraction angle, in degrees, corresponding to each peak in the XRD pattern). The calculated  $d$ -values are in good agreement with the data of JCPDS file No. 5-562 (the Joint Committee on Powder Diffraction Standards). The additional observed peak was attributed to the quartz substrate. The average crystallite size is estimated according to the Debye–Scherrer formula,  $D = \lambda K/B \cos\theta$ , where  $D$  is the average crystallite size,  $K$  is a constant,  $B$  is the full width at half maximum of the peaks,  $\lambda$  and  $\theta$  are defined above. Four  $\theta$  values corresponding to (111), (200), (220) and (311) plane are selected. The average crystallite size is  $15 \text{ \AA}$ .

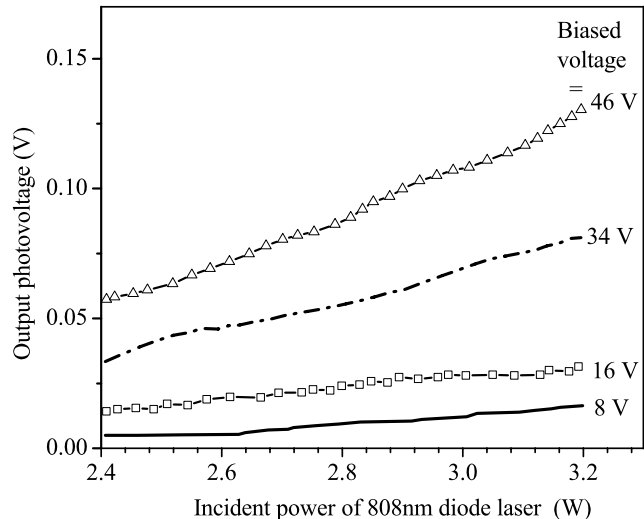


**Fig. 6** Response of PbS films to incident laser powers of  $808 \text{ nm}$  at different applied bias voltages

The surface morphology and structure of the deposited film are investigated in Fig. 2. The transmission electron microscope TEM images are presented in Fig. 2a, b. The resolution of TEM image (a) was taken at the scale of  $20 \text{ nm}$ . This image clearly shows that all the particles are easily distinguishable and are un-aggregated in the entire film. A localized TEM micrograph image of a higher resolution at scale  $5 \text{ nm}$  is shown in Fig. 2b. The shape of the deposited PbS nanocrystals is very regular square shape with curved corners. This shape was attributed to the cubic crystal structure. The scanning electron microscope SEM is depicted in

Fig. 2c. The SEM picture shows that the surface of the film is smooth and uniform with no observed cracks or deficiencies. Also, the selected area electron diffraction SAED pattern is presented in Fig. 2d. This SAED pattern confirms the XRD results of crystal structure of the deposited film.

Figures 3 and 4 show the absorption and emission spectra of the deposited PbS thin films of thicknesses 175 and 60 nm.

A blue shift is observed in the absorption spectra from 1000 nm to 800 nm as the film thickness decreased from 175 to 60 nm. This was attributed to the quantum confinement effect of the charge carriers in the restricted volume of thin films.

The blue shift is also observed in the emission spectra of the nano-size PbS films relative to the normal IR emission at 3200 nm in case of bulk PbS. The blue shift increased from 1100 nm to 1000 nm as the film thickness decreases from 175 nm to 60 nm (Fig. 4).

*I–V* characteristics of nano-structured PbS film and bulk samples are shown in Fig. 5(a, b) at three values of temperatures, namely: 20°C, 50°C and 80°C. The current increases linearly to a saturation value for both of the bulk and the film samples. The film samples show much higher values of resistance than the bulk samples.

The photoconductivity of the nano-structured PbS film was examined at room temperature. The response of the films to photons in the NIR region is presented in Fig. 6. The output voltage increases linearly with the incident powers of 808 nm laser diode at different values of the applied bias. Better response of PbS films is observed at higher values of applied bias.

#### 4 Conclusion

PbS nanostructure have been grown on a quartz substrate by PLD technique by ablating pure PbS bulk target. Films with different thicknesses were produced by varying the deposition time. Homogeneous surface morphology of magic-square-shaped nanocrystals has been proven for the deposited films by TEM, SEM, SAED and XRD analysis. The absorption and emission data of the nanostructure PbS thin films show a blue shift from the corresponding normal data for PbS bulk material. The blue shift increased as the film thickness decreased due to confinement effect. Linear increase was observed in the *I–V* characteristic for both PbS film and bulk samples. Much higher resistance values are measured for the nanocrystal PbS films. The photoconductivity of the films shows a linear response to the NIR photons. Better response is observed at higher bias voltages.

#### References

1. P. Gadenne, Y. Yagil, G. Deutscher, *J. Appl. Phys.* **66**, 3019 (1989)
2. A. Lee, in *SPIE*, vol. 3857, p. 92 (1998)
3. P.K. Nair, O. Gomezdaza, M.T. Nair, *Adv. Mater. Opt. Electron.* **1**, 139 (1992)
4. T.K. Chaudhuri, S. Chatterjee, *Proc. Int. Conf. Thermoelectr.* **11**, 40 (1992)
5. F.C. Meldrum, J. Flath, W. Knoll, *Thin Solid Films* **348**, 188 (1999)
6. V. Sukhovatkin, S. Musikhin, I. Gorelikov, S. Cauchi, L. Bakueva, E. Kumacheva, E.H. Sargent, *Opt. Lett.* **30**, 171 (2005)
7. J. Schubert, M.J. Schonung, Yu.G. Mourzina, A.V. Legin, Yu.G. Vlasov, W. Zander, H. Luth, *Sens. Actuators B, Chem.* **76**, 327 (2001)
8. P. Yang, C.F. Song, M.K. Lu, X. Yin, G.J. Zhou, D. Xu, D.R. Yuan, *Chem. Phys. Lett.* **345**, 429 (2001)
9. Y. Wang, *Acc. Chem. Res.* **24**, 133 (1991)
10. R.S. Kane, R.E. Cohen, R. Silbey, *J. Phys. Chem.* **100**, 7928 (1996)
11. F.M. Livingstone, W. Duncan, T. Baird, *J. Appl. Phys.* **48**, 3807 (1977)
12. V.I. Levchenko, L.I. Postnova, V.P. Bondarenko, N.N. Vorozov, V.A. Yakovtseva, L.N. Dolgy, *Thin Solid Films* **348**, 141 (1999)
13. S. Hashimoto, N. Koguchi, S. Takahashi, S. Akiba, *J. Cryst. Growth* **2**, 599 (1989)
14. T. Kanniainen, S. Lindroos, J. Ihanus, M. Leskela, *J. Mater. Chem.* **6**, 161 (1996)
15. T. Kanniainen, S. Lindroos, R. Resch, M. Leskela, G. Friedbacher, M. Grasserbauer, *Mater. Res. Bull.* **35**, 1045 (2000)
16. J. Puiso, S. Lindroos, S. Tamulevicius, M. Leskela, V. Snitka, *Thin Solid Films* **428**, 223 (2003)
17. M. Takahashi, Y. Ohshima, K. Nagata, S. Furuta, *J. Electroanal. Chem.* **359**, 281 (1993)
18. H. Saloniemi, M. Ritala, M. Leskela, R. Lappalainen, *J. Electrochem. Soc.* **146**, 2522 (1999)
19. S.I. Sadovnikov, A.I. Gusev, A.A. Rempel, *JETP Lett.* **89**, 238 (2009)
20. B. Thangaraju, P. Kaliannan, *Semicond. Sci. Technol.* **15**, 849 (2000)
21. R.S. Patil, H.M. Pathan, T.P. Gujar, C.D. Lokhande, *J. Mater. Sci.* **41**, 5723 (2006)
22. K.M. Gadave, S.A. Jodgudri, C.D. Lokhande, *Thin Solid Films* **245**, 7 (1994)
23. M. Xi, H. Xie, J. Zheng, Z.L. Wu, J. Li, G.Z. Zhao, *IR spaceborne remote sensing*, in *SPIE Proc.*, vol. 3122, p. 420 (1997)
24. J. Vaitkus, V. Kazlauskienė, J. Miskinis, J. Sinius, *Mater. Res. Bull.* **33**, 711 (1998)
25. J. Schubert, M.J. Schonung, Yu.G. Mourzina, A.V. Legin, Yu.G. Vlasov, W. Zander, H. Luth, *Sens. Actuators B, Chem.* **76**, 327 (2001)
26. M.S. Dhlamini, J.J. Terblans, O.M. Ntwaeborwa, J.M. Ngaruiya, K.T. Hillie, J.R. Botha, H.C. Swart, *J. Lumin.* **128**, 1997 (2008)
27. S. Kumar, R. Chandra, *Chalcogenide Lett.* **6**, 273 (2009)